

CMM-SolMech 2022

Vibrations of an Orthotropic Plate with Point Supports Subjected to a Moving Force

Filip ZAKĘŚ 

*Wroclaw University of Environmental and Life Sciences
The Faculty of Environmental Engineering and Geodesy
Wroclaw, Poland; e-mail: filip.zakes@upwr.edu.pl*

We investigate the dynamic behavior of a rectangular orthotropic plate loaded with the concentrated force moving with constant speed along the structure. In this work, we consider two types of plates in terms of boundary conditions. In the first case, we assume that the plate is simply supported on all of its edges with a number of point supports arbitrarily located in its area, and in the second one, we look at a two-span bridge plate with arbitrarily oriented intermediate linear support. Solutions for both cases are obtained by replacing the original structure with a single-span plate subjected to a given moving load and redundant forces situated in positions of removed intermediate supports. Redundant forces are obtained by the application of Volterra integral equations for the simply supported plate, and finite difference discretization and the Newmark method for the bridge plate. Two numerical examples are given to prove the effectiveness of the presented approach.

Keywords: orthotropic plate; moving load; vibrations; Volterra integral equations.

1. INTRODUCTION

Many types of structures are subjected to various types of moving loads causing structural vibrations. It is a problem that occurs, for example, in road and railway bridges, ceilings above underground passages, tunnels, or runways. This issue was analyzed by many authors for many years with various types of structures as well as different moving load models taken into account [2, 7, 11, 12]. In civil engineering, structures such as bridges or ceilings can be effectively modeled as rectangular orthotropic plates. Structural orthotropy occurs in slabs stiffened with uni- or bidirectional ribs, grillages, box floors, and slabs on trapezoidal plates or plates made of orthotropic material (for example, wood). LANGER [4] proposed a solution for the eigenvalue problem of the orthotropic bridge plate by applying the Ritz method and Legendre's polyno-

mials. KLASZTORNY [3] analyzed damped vibrations of rectangular orthotropic bridge plate resulting from moving inertial loads, described by matrix differential equations of Hill's type. LAW *et al.* [6] obtained the dynamic response of a bridge deck subjected to moving loads by applying Hamilton's principle and modal superposition. PAPKOV [10] proposed an asymptotically exact solution for the problem of transverse vibrations of rectangular orthotropic plate with free edges. ZHANG and ZHANG [13] applied the method of finite integral transforms to solve the problem of the transverse vibration of a plate with two opposite edges rotationally restrained. MARTÍNEZ-RODRIGO *et al.* [9] investigated the dynamic response of railway bridges modeled as orthotropic plates simply- or elastically supported on opposite edges in terms of free vibrations and vibrations resulting from a stream of moving constant forces. FARAH *et al.* [1] proposed a semi-analytical solution based on modal superposition for the free vibration problem of a multi-span orthotropic bridge plate with rubber bearings. LENARTOWICZ and GUMINIAK [8] applied the finite element method and finite difference method to describe free vibrations of iso- and orthotropic plates with variable thickness and contact with water taken into account.

This work is focused on two types of orthotropic plates. The first one is a plate of dimensions B and L simply supported on all its edges and point supported by a number of k intermediate supports (see Fig. 1). The second one is a plate with two simply supported and two free edges with arbitrarily oriented intermediate linear support dividing the plate into two spans (see Fig. 2). Both plates are subjected to the concentrated force of magnitude P moving along the plate with constant speed v .

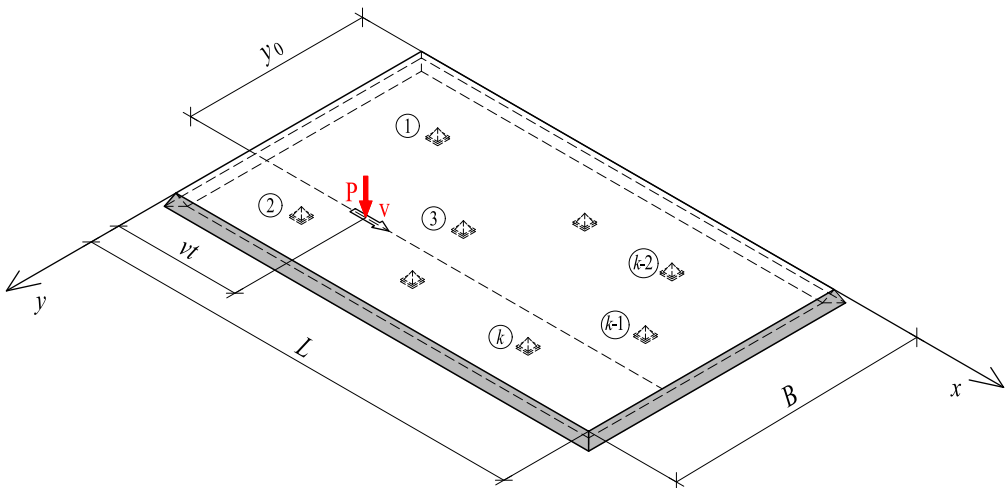


FIG. 1. Simply supported plate with point supports subjected to a moving force.

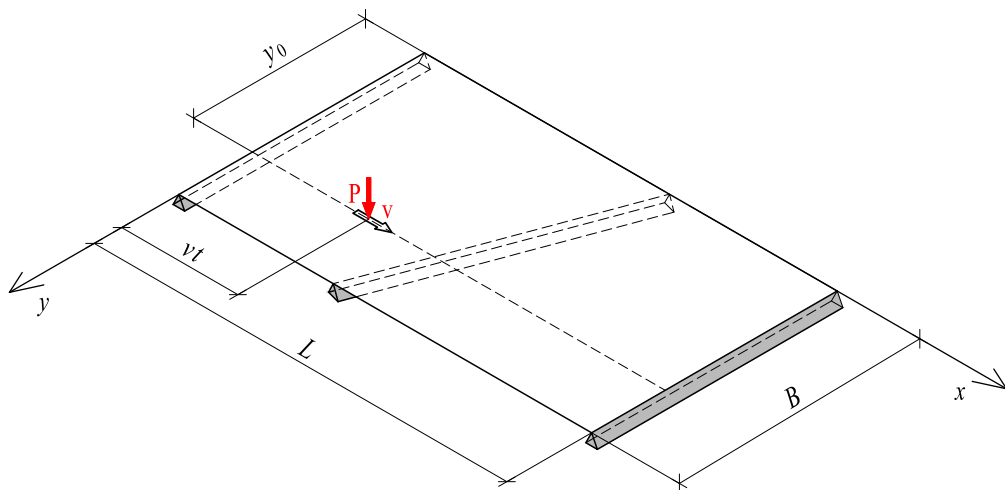


FIG. 2. Two-span bridge plate subjected to a moving force.

Equation of motion describing vibrations $w = w(x, y, t)$ of an orthotropic plate subjected to a force P moving with speed v on the distance y_0 measured from the axis x has the form

$$(1.1) \quad D_x \frac{\partial^4 w}{\partial x^4} + 2H \frac{\partial^4 w}{\partial x^2 \partial y^2} + D_y \frac{\partial^4 w}{\partial y^4} + \mu \ddot{w} = P \delta(x - vt) \delta(y - y_0),$$

where D_x and D_y are the flexural rigidities in the x - and y -directions, $H = D_1 + 2D_{xy}$ is the effective torsional rigidity, where $D_1 = \nu_y D_x = \nu_x D_y$ is defined with Poisson's ratios ν_x and ν_y , D_{xy} is the torsional rigidity, and μ is the mass of the plate per unit area. Symbol δ on the right side of Eq. (1.1) denotes the Dirac delta.

2. SIMPLY SUPPORTED PLATE WITH POINT SUPPORTS

As the first type of structure, we shall consider a simply supported rectangular plate of length L and width B with a number of k arbitrarily situated point supports. In the presented approach, we replace this model with a simply supported plate subjected to a given moving load and point time-varying forces $X_i(t)$ applied at positions of removed intermediate supports (see Fig. 3).

2.1. Case of a moving constant force

The equation of motion for the plate loaded with a force moving with constant speed has the form (1.1). Boundary conditions for the plate simply supported on all edges are

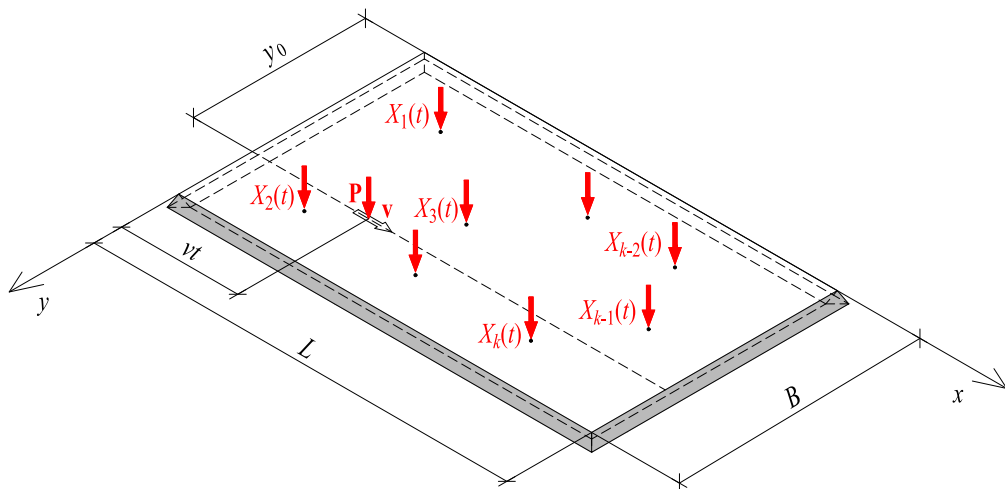


FIG. 3. Simply supported plate subjected to a moving force and concentrated time-varying forces.

$$\begin{aligned}
 w(0, y, t) &= w(L, y, t) = 0, \\
 w(x, 0, t) &= w(x, B, t) = 0, \\
 (2.1) \quad \frac{\partial^2 w(x, y, t)}{\partial x^2} \Big|_{x=0} &= \frac{\partial^2 w(x, y, t)}{\partial x^2} \Big|_{x=L} = 0, \\
 \frac{\partial^2 w(x, y, t)}{\partial y^2} \Big|_{y=0} &= \frac{\partial^2 w(x, y, t)}{\partial y^2} \Big|_{y=B} = 0,
 \end{aligned}$$

and the initial conditions are

$$(2.2) \quad w(x, y, 0) = \dot{w}(x, y, 0) = 0.$$

We assume the solution in the form of double sine series:

$$(2.3) \quad w^P(x, y, t) = \sum_{m=1}^{\infty} \sum_{n=1}^{\infty} Y_{mn}(t) \sin \frac{m\pi x}{L} \sin \frac{n\pi y}{B}.$$

After substituting expression (2.3) into Eq. (1.1) and applying the orthogonality method, we obtain a set of ordinary differential equations:

$$(2.4) \quad \ddot{Y}_{mn}(t) + \omega_{mn}^2 Y_{mn}(t) = \frac{4P}{\mu BL} \sin \frac{m\pi vt}{L} \sin \frac{n\pi y_0}{B},$$

where

$$(2.5) \quad \omega_{mn}^2 = \frac{1}{\mu} \left[D_x \left(\frac{m\pi}{L} \right)^4 + 2H \left(\frac{m\pi}{L} \right)^2 \left(\frac{n\pi}{B} \right)^2 + D_y \left(\frac{n\pi}{B} \right)^4 \right].$$

Assuming zero initial conditions, function $Y_{mn}(t)$ can be presented as

$$(2.6) \quad Y_{mn}(t) = \frac{4P}{\mu BL} \left[\frac{\sin \frac{m\pi vt}{L} \sin \frac{n\pi y_0}{B}}{\omega_{mn}^2 - \left(\frac{m\pi v}{L} \right)^2} - \frac{\frac{m\pi v}{L} \sin \frac{m\pi vt}{L} \sin \frac{n\pi y_0}{B}}{\omega_{mn} \left[\omega_{mn}^2 - \left(\frac{m\pi v}{L} \right)^2 \right]} \right].$$

Therefore, vibrations of the plate resulting from the moving force have the following form:

$$(2.7) \quad w^P(x, y, t) = \frac{4P}{\mu BL} \left[\sum_{m=1}^{\infty} \sum_{n=1}^{\infty} \frac{\sin \frac{m\pi vt}{L} \sin \frac{n\pi y_0}{B} \sin \frac{m\pi x}{L} \sin \frac{n\pi y}{B}}{\omega_{mn}^2 - \left(\frac{m\pi v}{L} \right)^2} - \sum_{m=1}^{\infty} \sum_{n=1}^{\infty} \frac{\frac{m\pi v}{L} \sin \frac{m\pi vt}{L} \sin \frac{n\pi y_0}{B} \sin \frac{m\pi x}{L} \sin \frac{n\pi y}{B}}{\omega_{mn} \left[\omega_{mn}^2 - \left(\frac{m\pi v}{L} \right)^2 \right]} \right].$$

2.2. Case of a concentrated time-varying force

The equation of motion for the plate loaded with the concentrated time-varying force $X_i(t)$ situated at coordinates x_i, y_i has the following form:

$$(2.8) \quad D_x \frac{\partial^4 w}{\partial x^4} + 2H \frac{\partial^4 w}{\partial x^2 \partial y^2} + D_y \frac{\partial^4 w}{\partial y^4} + \mu \ddot{w} = X_i(t) \delta(x - x_i) \delta(y - y_i).$$

The solution of Eq. (2.9) has a similar form as for Eq. (1.1):

$$(2.9) \quad w^{X_i}(x, y, t) = \sum_{m=1}^{\infty} \sum_{n=1}^{\infty} Y_{mn}(t) \sin \frac{m\pi x}{L} \sin \frac{n\pi y}{B}.$$

Substituting expression (2.9) into Eq. (1.1) and using the orthogonality method, we obtain a set of ordinary differential equations

$$(2.10) \quad \ddot{Y}_{mn}(t) + \omega_{mn}^2 Y_{mn}(t) = \frac{4}{\mu BL} X_i(t) \sin \frac{m\pi x_i}{L} \sin \frac{n\pi y_i}{B},$$

where ω_{mn}^2 is described as (2.5). The solution of Eq. (2.10) can be presented in the convolution form:

$$(2.11) \quad Y_{mn}(t) = \frac{4}{\mu BL} \sin \frac{m\pi x_i}{L} \sin \frac{n\pi y_i}{B} \int_0^t h_{mn}(t - \tau) X_i(\tau) d\tau,$$

where $h_{mn}(t)$ is the impulse response function described as

$$(2.12) \quad h_{mn}(t) = \frac{1}{\omega_{mn}} \sin \omega_{mn} t.$$

Finally, vibrations of the plate have the following form:

$$(2.13) \quad w^{X_i}(x, y, t) = \frac{4}{\mu BL} \sum_{m=1}^{\infty} \sum_{n=1}^{\infty} \sin \frac{m\pi x_i}{L} \sin \frac{n\pi y_i}{B} \cdot \sin \frac{m\pi x}{L} \sin \frac{n\pi y}{B} \int_0^t \frac{1}{\omega_{mn}} \sin \omega_{mn}(t - \tau) X_i(\tau) d\tau.$$

2.3. Vibrations of a plate with point supports

Vibrations of a simply supported plate with k point supports can be presented through the superposition of previously solved cases:

$$(2.14) \quad w(x, y, t) = \sum_{i=1}^k w^{X_i}(x, y, t) + w^P(x, y, t).$$

Knowing that deflections of the plate at the positions of point supports are equal to 0, we can build a system of Volterra integral equations of the first kind in order to find functions $X_i(t)$ describing reactions on the point supports:

$$(2.15) \quad \sum_{i=1}^k \int_0^T d_{ij}(t - \tau) X_j(\tau) d\tau + \Delta_{iP}(t) = 0, \quad j = 1, 2, \dots, k,$$

where

$$(2.16) \quad d_{ij}(t) = \frac{4}{\mu BL} \sum_{m=1}^{\infty} \sum_{n=1}^{\infty} h_{mn}(t) \sin \frac{m\pi x_i}{L} \sin \frac{n\pi y_i}{B} \sin \frac{m\pi x_j}{L} \sin \frac{n\pi y_j}{B},$$

$$\Delta_{iP}(t) = w^P(x_i, y_i, t).$$

To avoid difficulties of solving a system of integral equations analytically, we shall apply a simple procedure in which we replace direct integration with a numerical one:

$$(2.17) \quad \int_0^{T_R} d_{ij}(t_R - \tau) X_j(\tau) d\tau = \sum_{r=1}^R d_{ij}(t_R - \tau_r) X_j(\tau_r) \Delta\tau.$$

The procedure above is based on the midpoint method in which we divide the time of force movement on the plate $t_{\max} = L/v$ into N equal time segments $\Delta\tau$. This way, we can replace Eq. (2.15) with

$$(2.18) \quad \sum_{j=1}^k \sum_{r=1}^R d_{ij}(t_R - \tau_r) X_j(\tau_r) \Delta\tau + \Delta_{iP}(t_R) = 0, \quad i = 1, 2, \dots, k,$$

where

$$(2.19) \quad \begin{aligned} t_R &= R\Delta\tau, & \tau_r &= (r - 0,5) \Delta\tau, & r &= 1, 2, \dots, R, \\ R &= 1, 2, \dots, N, & \Delta\tau &= L/(Nv). \end{aligned}$$

Time step $\Delta\tau$ used for the numerical calculations should be carefully selected in order to obtain an acceptable and stable solution. The size of time step $\Delta\tau$ depends on the highest value of ω_{mn} used in previous formulas and should fulfill the condition:

$$(2.20) \quad \Delta\tau < \frac{2\pi}{\omega_{mn,\max}}.$$

Further calculations were performed assuming $m_{\max} = n_{\max} = 10$. The convergence analysis proved that for higher values of m and n used in the series, differences in obtained results are negligible.

3. TWO-SPAN BRIDGE PLATE

As the second type of structure, we consider a two-span bridge plate with arbitrarily situated linear support dividing the plate into two spans. Similarly to the previous model, we remove intermediate support and introduce linear load $X(x, y, t)$ describing support reaction. Single-span bridge plate subjected to a given moving force P and distributed load $X(x, y, t)$ is shown in Fig. 4.

Boundary conditions for the bridge plate are

$$(3.1) \quad \begin{aligned} w(0, y, t) &= w(L, y, t) = 0, \\ \frac{\partial^2 w(x, y, t)}{\partial x^2} \Big|_{x=0} &= \frac{\partial^2 w(x, y, t)}{\partial x^2} \Big|_{x=L} = 0, \\ \frac{\partial^2 w(x, y, t)}{\partial y^2} \Big|_{y=0} &= \frac{\partial^2 w(x, y, t)}{\partial y^2} \Big|_{y=B} = 0, \\ \frac{\partial^3 w(x, y, t)}{\partial y^3} \Big|_{y=0} &= \frac{\partial^3 w(x, y, t)}{\partial y^3} \Big|_{y=B} = 0. \end{aligned}$$

Initial conditions are the same as for the simply supported plate – Eq. (2.2).

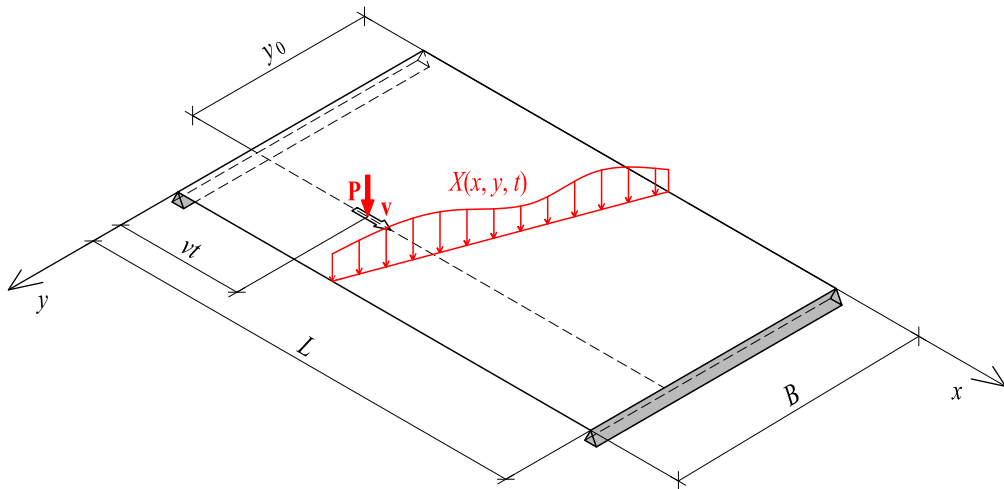


FIG. 4. Single-span bridge plate subjected to a moving force and distributed time-varying linear load.

3.1. Case of moving constant force

The solution of the equation of motion (1.1) for a simply supported bridge plate subjected to the moving force can be presented as

$$(3.2) \quad w^P(x, y, t) = \sum_{n=1}^{\infty} V_n(y, t) \sin \frac{n\pi x}{L}.$$

After substituting expression (3.2) into the equation of motion (1.1) and using the orthogonality method, we obtain a set of partial differential equations:

$$(3.3) \quad \mu \ddot{V}_n(y, t) + D_y \frac{\partial^4 V_n(y, t)}{\partial y^4} - 2H \left(\frac{n\pi}{L} \right)^2 \frac{\partial^2 V_n(y, t)}{\partial y^2} + D_x \left(\frac{n\pi}{L} \right)^4 V_n(y, t) = \frac{2P}{L} \sin \frac{n\pi vt}{L} \delta(y - y_0).$$

In order to replace partial differential equations with ordinary differential equations, we shall use central difference quotients:

$$(3.4) \quad \frac{\partial^2 V_n(y, t)}{\partial y^2} = \frac{1}{(\Delta y)^2} [V_{n,i-1}(t) - 2V_{n,i}(t) + V_{n,i+1}(t)],$$

$$\frac{\partial^4 V_n(y, t)}{\partial y^4} = \frac{1}{(\Delta y)^4} [V_{n,i-2}(t) - 4V_{n,i-1}(t) + 6V_{n,i}(t) - 4V_{n,i+1}(t) + V_{n,i+2}(t)].$$

Let us divide the plate into s longitudinal stripes (along axis x) of equal width Δy and apply formulas (3.4). This will lead us to ordinary differential equations:

$$(3.5) \quad \mu \ddot{V}_{n,i}^P(t) + A_n V_{n,i-2}^P(t) + B_n V_{n,i-1}^P(t) + C_n V_{n,i}^P(t) + B_n V_{n,i+1}^P(t) + A_n V_{n,i+2}^P(t) = P_{n,i}(t) \quad \text{for } i = 2, 3, \dots, s-2,$$

where constants A_n, B_n, C_n are described as

$$(3.6) \quad A_n = \frac{D_y}{(\Delta y)^4}, \quad B_n = - \left[\frac{4D_y}{(\Delta y)^4} + \frac{2H}{(\Delta y)^2} \left(\frac{n\pi}{L} \right)^2 \right],$$

$$C_n = \left[\frac{6D_y}{(\Delta y)^4} + \frac{4H}{(\Delta y)^2} \left(\frac{n\pi}{L} \right)^2 + D_x \left(\frac{n\pi}{L} \right)^4 \right]$$

equations for $i = 0, i = 1, i = s-1, i = s$ are related to boundary conditions (free edges at $y = 0$ and $y = B$)

$$(3.7) \quad \begin{aligned} \mu \ddot{V}_{n,0}^P(t) + D_n V_{n,0}^P(t) + E_n V_{n,1}^P(t) + F_n V_{n,2}^P(t) &= P_{n,0}(t) \\ &\text{for } i = 0, \\ \mu \ddot{V}_{n,0}^P(t) + G_n V_{n,0}^P(t) + H_n V_{n,1}^P(t) + B_n V_{n,2}^P(t) + A_n V_{n,3}^P(t) &= P_{n,1}(t) \\ &\text{for } i = 1, \\ \mu \ddot{V}_{n,s-1}^P(t) + A_n V_{n,s-3}^P(t) + B_n V_{n,s-2}^P(t) + H_n V_{n,s-1}^P(t) + G_n V_{n,s}^P(t) &= P_{n,s-1}(t) \\ &\text{for } i = s-1, \\ \mu \ddot{V}_{n,s}^P(t) + F_n V_{n,s-2}^P(t) + E_n V_{n,s-1}^P(t) + D_n V_{n,s}^P(t) &= P_{n,s}(t) \\ &\text{for } i = s, \end{aligned}$$

where constants D_n, E_n, F_n, G_n, H_n have the form:

$$(3.8) \quad \begin{aligned} D_n &= \frac{6D_y}{(\Delta y)^4} + \frac{4H}{(\Delta y)^2} \left(\frac{n\pi}{L} \right)^2 + D_x \left(\frac{n\pi}{L} \right)^4 \\ &\quad - \left[\frac{2D_y}{(\Delta y)^4} + \frac{H - 2D_{xy}}{(\Delta y)^2} \left(\frac{n\pi}{L} \right)^2 \right] \left[2 + (\Delta y)^2 \nu_x \left(\frac{n\pi}{L} \right)^2 \right], \\ E_n &= - \frac{2D_y}{(\Delta y)^4} \left[2 + (\Delta y)^2 \frac{H + 2D_{xy}}{D_y} \left(\frac{n\pi}{L} \right)^2 \right], \\ F_n &= \frac{2D_y}{(\Delta y)^4}, \quad G_n = - \left[\frac{2D_y}{(\Delta y)^4} + \frac{2H - \nu_x D_y}{(\Delta y)^2} \left(\frac{n\pi}{L} \right)^2 \right], \\ H_n &= \frac{5D_y}{(\Delta y)^4} + \frac{4H}{(\Delta y)^2} \left(\frac{n\pi}{L} \right)^2 + D_x \left(\frac{n\pi}{L} \right)^4. \end{aligned}$$

Equations (3.5) and (3.7) can be presented in the matrix notation:

$$(3.9) \quad \mathbf{M} \cdot \ddot{\mathbf{V}}^P(t) + \mathbf{K} \cdot \mathbf{V}^P(t) = \mathbf{P}(t).$$

Taking into account a number of N mode shape functions, the vectors of displacements and accelerations will be presented as

$$(3.10) \quad \mathbf{V}^P(t) = \begin{bmatrix} \mathbf{V}_1^P(t) \\ \mathbf{V}_2^P(t) \\ \vdots \\ \mathbf{V}_N^P(t) \end{bmatrix}, \quad \mathbf{V}_n^P(t) = \begin{bmatrix} V_{n,0}^P(t) \\ V_{n,1}^P(t) \\ \vdots \\ V_{n,s}^P(t) \end{bmatrix},$$

$$\ddot{\mathbf{V}}^P(t) = \begin{bmatrix} \ddot{\mathbf{V}}_1^P(t) \\ \ddot{\mathbf{V}}_2^P(t) \\ \vdots \\ \ddot{\mathbf{V}}_N^P(t) \end{bmatrix}, \quad \ddot{\mathbf{V}}_n^P(t) = \begin{bmatrix} \ddot{V}_{n,0}^P(t) \\ \ddot{V}_{n,1}^P(t) \\ \vdots \\ \ddot{V}_{n,s}^P(t) \end{bmatrix}, \quad n = 1, 2, \dots, N.$$

The mass matrix \mathbf{M} will have diagonal form:

$$(3.11) \quad \mathbf{M} = \begin{bmatrix} \mathbf{M}_1 & & & \\ & \mathbf{M}_2 & & \\ & & \ddots & \\ & & & \mathbf{M}_N \end{bmatrix}_{N(s+1) \times N(s+1)},$$

$$\mathbf{M}_n = \begin{bmatrix} \mu/2 & & & \\ & \mu & & \\ & & \ddots & \\ & & & \mu/2 \end{bmatrix}_{(s+1) \times (s+1)}.$$

The stiffness matrix \mathbf{K} will be presented as

$$(3.12) \quad \mathbf{K} = \begin{bmatrix} \mathbf{K}_1 & & & \\ & \mathbf{K}_2 & & \\ & & \ddots & \\ & & & \mathbf{K}_N \end{bmatrix}_{N(s+1) \times N(s+1)},$$

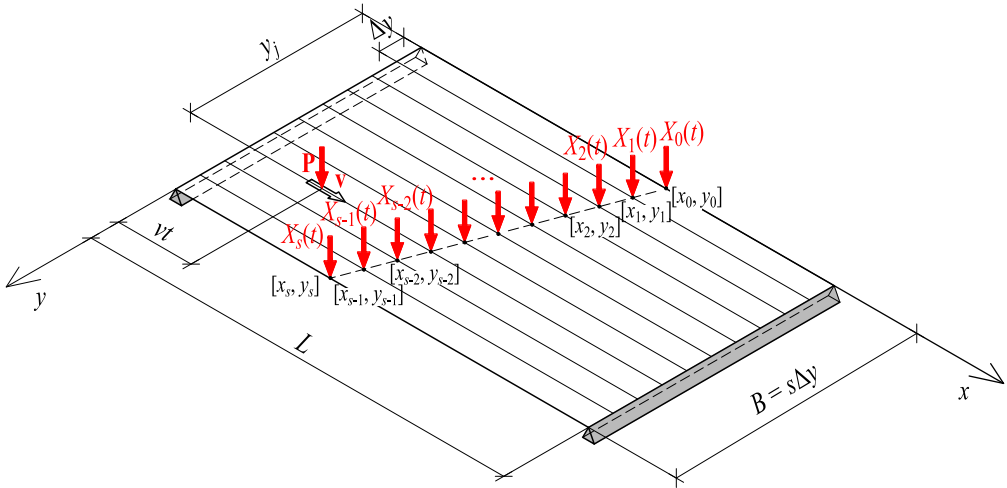


FIG. 5. Single-span bridge plate subjected to concentrated time-varying forces situated on the line of intermediate support.

Ordinary differential equations obtained by applying finite difference procedures have the form:

$$\begin{aligned}
 \mu \ddot{V}_{n,0}^X(t) + D_n V_{n,0}^X(t) + E_n V_{n,1}^X(t) + F_n V_{n,2}^X(t) &= X_{n,0}(t) && \text{for } i = 0, \\
 \mu \ddot{V}_{n,0}^X(t) + G_n V_{n,0}^X(t) + H_n V_{n,1}^X(t) + B_n V_{n,2}^X(t) + A_n V_{n,3}^X(t) &= X_{n,1}(t) && \text{for } i = 1, \\
 \mu \ddot{V}_{n,i}^X(t) + A_n V_{n,i-2}^X(t) + B_n V_{n,i-1}^X(t) + C_n V_{n,i}^X(t) &+ B_n V_{n,i+1}^X(t) + A_n V_{n,i+2}^X(t) &= X_{n,i}(t) && \text{for } i = 2, 3, \dots, s-2, \\
 \mu \ddot{V}_{n,s-1}^X(t) + A_n V_{n,s-3}^X(t) + B_n V_{n,s-2}^X(t) + H_n V_{n,s-1}^X(t) &+ G_n V_{n,s}^X(t) &= X_{n,s-1}(t) && \text{for } i = s-1, \\
 \mu \ddot{V}_{n,s}^X(t) + F_n V_{n,s-2}^X(t) + E_n V_{n,s-1}^X(t) + D_n V_{n,s}^X(t) &= X_{n,s}(t) && \text{for } i = s.
 \end{aligned}
 \tag{3.17}$$

Constants A_n, \dots, H_n are described by formulas (3.6) and (3.8). The matrix notation for the equations above has the form:

$$\mathbf{M} \cdot \ddot{\mathbf{V}}^X(t) + \mathbf{K} \cdot \mathbf{V}^X(t) = \mathbf{X}(t),
 \tag{3.18}$$

where mass and stiffness matrices are described as (3.11) and (3.12). Vectors of displacements and accelerations can be presented as

$$(3.19) \quad \mathbf{V}^X(t) = \begin{bmatrix} \mathbf{V}_1^X(t) \\ \mathbf{V}_2^X(t) \\ \vdots \\ \mathbf{V}_N^X(t) \end{bmatrix}, \quad \mathbf{V}_n^X(t) = \begin{bmatrix} V_{n,0}^X(t) \\ V_{n,1}^X(t) \\ \vdots \\ V_{n,s}^X(t) \end{bmatrix},$$

$$\ddot{\mathbf{V}}^P(t) = \begin{bmatrix} \ddot{\mathbf{V}}_1^X(t) \\ \ddot{\mathbf{V}}_2^X(t) \\ \vdots \\ \ddot{\mathbf{V}}_N^X(t) \end{bmatrix}, \quad \ddot{\mathbf{V}}_n^P(t) = \begin{bmatrix} \ddot{V}_{n,0}^X(t) \\ \ddot{V}_{n,1}^X(t) \\ \vdots \\ \ddot{V}_{n,s}^X(t) \end{bmatrix}, \quad n = 1, 2, \dots, N.$$

The load vector has the form:

$$(3.20) \quad \mathbf{X}(t) = \begin{bmatrix} \mathbf{X}_1(t) \\ \mathbf{X}_2(t) \\ \vdots \\ \mathbf{X}_N(t) \end{bmatrix}, \quad \mathbf{X}_n(t) = \begin{bmatrix} X_{n,0}(t) \\ X_{n,1}(t) \\ \vdots \\ X_{n,s}(t) \end{bmatrix},$$

where

$$(3.21) \quad X_{n,i}(t) = \frac{2X_i(t)}{\Delta y L} \sin \frac{n\pi x_i}{L} \quad \text{for } i \neq 0 \quad \text{and } i \neq s,$$

$$X_{n,i}(t) = \frac{X_i(t)}{\Delta y L} \sin \frac{n\pi x_i}{L} \quad \text{for } i = 0 \quad \text{or } i = s.$$

3.3. Two-span bridge plate

The solution for a two-span bridge plate is obtained by combining two previously analyzed cases and applying the Newmark method formulas [5] for the case of moving constant force:

$$(3.22) \quad \mathbf{V}^P(t_{r+1}) = \mathbf{V}^P(t_r) + \Delta t \dot{\mathbf{V}}^P(t_r) + \alpha (\Delta t)^2 \ddot{\mathbf{V}}^P(t_r) + \beta (\Delta t)^2 \ddot{\mathbf{V}}^P(t_{r+1}),$$

$$\dot{\mathbf{V}}^P(t_{r+1}) = \dot{\mathbf{V}}^P(t_r) + \frac{1}{2} \Delta t \ddot{\mathbf{V}}^P(t_r) + \frac{1}{2} \Delta t \ddot{\mathbf{V}}^P(t_{r+1}),$$

$$\ddot{\mathbf{V}}^P(t_{r+1}) = \widetilde{M}^{-1} \widetilde{\mathbf{P}}(t_{r+1}),$$

$$\widetilde{\mathbf{P}}(t_{r+1}) = \mathbf{P}(t_{r+1}) - \mathbf{K} \left[\mathbf{V}^P(t_r) + \Delta t \dot{\mathbf{V}}^P(t_r) + \alpha (\Delta t)^2 \ddot{\mathbf{V}}^P(t_r) \right],$$

and for the case of concentrated time-varying forces situated on the support line:

$$\begin{aligned}
 \mathbf{V}^X(t_{r+1}) &= \mathbf{V}^X(t_r) + \Delta t \dot{\mathbf{V}}^X(t_r) + \alpha (\Delta t)^2 \ddot{\mathbf{V}}^X(t_r) + \beta (\Delta t)^2 \ddot{\mathbf{V}}^X(t_{r+1}), \\
 \dot{\mathbf{V}}^X(t_{r+1}) &= \dot{\mathbf{V}}^X(t_r) + \frac{1}{2} \Delta t \ddot{\mathbf{V}}^X(t_r) + \frac{1}{2} \Delta t \ddot{\mathbf{V}}^X(t_{r+1}), \\
 \ddot{\mathbf{V}}^X(t_{r+1}) &= \widetilde{\mathbf{M}}^{-1} \widetilde{\mathbf{X}}(t_{r+1}), \\
 \widetilde{\mathbf{X}}(t_{r+1}) &= \mathbf{X}(t_{r+1}) - \mathbf{K} \left[\mathbf{V}^X(t_r) + \Delta t \dot{\mathbf{V}}^X(t_r) + \alpha (\Delta t)^2 \ddot{\mathbf{V}}^X(t_r) \right],
 \end{aligned}
 \tag{3.23}$$

where $r = 0, 1, \dots, R$. R is the number of time steps used in the Newmark numerical integration. For further calculations, the average acceleration method has been chosen with parameters $\beta = 0.25$ and $\alpha = 0.5 - \beta = 0.25 = \beta$ providing unconditional stability. Initial conditions are

$$\begin{aligned}
 \mathbf{V}^P(t_0 = 0) &= \mathbf{0}, & \dot{\mathbf{V}}^P(t_0 = 0) &= \mathbf{0}, & \ddot{\mathbf{V}}^P(t_0 = 0) &= \mathbf{0}, \\
 \mathbf{V}^X(t_0 = 0) &= \mathbf{0}, & \dot{\mathbf{V}}^X(t_0 = 0) &= \mathbf{0}, & \ddot{\mathbf{V}}^X(t_0 = 0) &= \mathbf{0}.
 \end{aligned}
 \tag{3.24}$$

The matrix $\widetilde{\mathbf{M}}$ required to determine the vector of accelerations unknown at every time step is described as

$$\begin{aligned}
 \widetilde{\mathbf{M}} &= \mathbf{M} + \beta (\Delta t)^2 \mathbf{K}, \\
 \widetilde{\mathbf{M}}^{-1} &= \left(\mathbf{M} + \beta (\Delta t)^2 \mathbf{K} \right)^{-1}, \\
 \widetilde{\mathbf{M}}^{-1} &= \begin{bmatrix} \widetilde{\mathbf{M}}_1^{-1} & & & \\ & \widetilde{\mathbf{M}}_2^{-1} & & \\ & & \ddots & \\ & & & \widetilde{\mathbf{M}}_N^{-1} \end{bmatrix}_{N(s+1) \times N(s+1)}, \\
 \widetilde{\mathbf{M}}_n^{-1} &= \begin{bmatrix} m_{n,00} & m_{n,01} & \cdots & m_{n,0s} \\ m_{n,10} & m_{n,11} & \cdots & m_{n,1s} \\ \vdots & \vdots & \ddots & \vdots \\ m_{n,s0} & m_{n,s1} & \cdots & m_{n,ss} \end{bmatrix}_{(s+1) \times (s+1)} = \begin{bmatrix} \mathbf{m}_{n,0}^T \\ \mathbf{m}_{n,1}^T \\ \vdots \\ \mathbf{m}_{n,s}^T \end{bmatrix}, \\
 \mathbf{m}_{n,i}^T &= [m_{n,i0} \ m_{n,i1} \ \cdots \ m_{n,is}].
 \end{aligned}
 \tag{3.25}$$

The vector \mathbf{X}^* containing values of forces $X_i(t)$ can be obtained from the system of compatibility equations given in the matrix form:

$$(3.26) \quad \mathbf{B} \cdot \mathbf{X}^*(t_{r+1}) + \mathbf{b}(t_{r+1}) = \mathbf{0}.$$

The matrix \mathbf{B} has the form:

$$(3.27) \quad \mathbf{B} = \frac{2\alpha (\Delta t)^2}{\Delta y L} \sum_{n=1}^N \left\{ \sin \frac{n\pi x_i}{L} \right\} \widetilde{\mathbf{M}}_n^{-1} \left\{ \sin \frac{n\pi x_i}{L} \right\},$$

where

$$(3.28) \quad \left\{ \sin \frac{n\pi x_i}{L} \right\} = \text{diag} \left(\sin \frac{n\pi x_0}{L}; \quad \sin \frac{n\pi x_1}{L}; \quad \dots; \quad \sin \frac{n\pi x_s}{L} \right).$$

The vector $\mathbf{b}(t_{r+1})$ is defined as

$$(3.29) \quad \mathbf{b}(t_{r+1}) = \begin{bmatrix} w_0^P(x_0, t_{r+1}) + \sum_{n=1}^N \sin \frac{n\pi x_0}{L} d_{n,0}(t_{r+1}) \\ w_1^P(x_1, t_{r+1}) + \sum_{n=1}^N \sin \frac{n\pi x_1}{L} d_{n,1}(t_{r+1}) \\ \vdots \\ w_s^P(x_s, t_{r+1}) + \sum_{n=1}^N \sin \frac{n\pi x_s}{L} d_{n,s}(t_{r+1}) \end{bmatrix},$$

where

$$(3.30) \quad \mathbf{d}_n(t_{r+1}) = \mathbf{V}_n^X(t_r) + \Delta t \dot{\mathbf{V}}_n^X(t_r) + \alpha (\Delta t)^2 \left[\ddot{\mathbf{V}}_n^X(t_r) - \mathbf{u}_n(t_{r+1}) \right] \\ = \begin{bmatrix} d_{n,0}(t_{r+1}) \\ d_{n,1}(t_{r+1}) \\ \vdots \\ d_{n,s}(t_{r+1}) \end{bmatrix}$$

and

$$(3.31) \quad \mathbf{u}_n(t_{r+1}) = \begin{bmatrix} \mathbf{m}_{n,0}^T \cdot [\mathbf{K} \cdot \mathbf{V}_n^X(t_{r+1})] \\ \mathbf{m}_{n,1}^T \cdot [\mathbf{K} \cdot \mathbf{V}_n^X(t_{r+1})] \\ \vdots \\ \mathbf{m}_{n,s}^T \cdot [\mathbf{K} \cdot \mathbf{V}_n^X(t_{r+1})] \end{bmatrix}.$$

The vector \mathbf{X}^* can then be defined as

$$(3.32) \quad \mathbf{X}^*(t_{r+1}) = -\mathbf{B}^{-1} \cdot \mathbf{b}(t_{r+1}) = \begin{bmatrix} X_0(t_{r+1}) \\ X_1(t_{r+1}) \\ \vdots \\ X_s(t_{r+1}) \end{bmatrix}.$$

The load vector in Eq. (3.16) has the form:

$$(3.33) \quad \mathbf{X}(t_{r+1}) = \begin{bmatrix} \mathbf{X}_1(t_{r+1}) \\ \mathbf{X}_2(t_{r+1}) \\ \vdots \\ \mathbf{X}_N(t_{r+1}) \end{bmatrix}, \quad \mathbf{X}_n(t_{r+1}) = \begin{bmatrix} X_{n,0}(t_{r+1}) \\ X_{n,1}(t_{r+1}) \\ \vdots \\ X_{n,s}(t_{r+1}) \end{bmatrix},$$

where

$$(3.34) \quad X_{n,i}(t_{r+1}) = \frac{2X_i(t_{r+1})}{\Delta y L} \sin \frac{n\pi x_i}{L} \quad \text{for } i \neq 0 \text{ and } i \neq s,$$

$$X_{n,i}(t_{r+1}) = \frac{X_i(t_{r+1})}{\Delta y L} \sin \frac{n\pi x_i}{L} \quad \text{for } i = 0 \text{ or } i = s.$$

Finally, vibrations of the two-span bridge plate can be presented as

$$(3.35) \quad w(x, y_i, t_r) = w^P(x, y_i, t_r) + w^X(x, y_i, t_r)$$

$$= \sum_{n=1}^N \sin \frac{n\pi x}{L} V_{n,i}^P(t_r) + \sum_{n=1}^N \sin \frac{n\pi x}{L} V_{n,i}^X(t_r).$$

4. NUMERICAL EXAMPLES

4.1. Simply supported plate with two point supports

The first presented example is of a simply supported rectangular orthotropic plate with two point supports of dimensions shown in Fig. 6. Plate rigidities are equal to $D_x = 7.68 \cdot 10^8 \text{ N} \cdot \text{m}$, $D_y = H = 1.82 \cdot 10^8 \text{ N} \cdot \text{m}$, $D_{xy} = 7.29 \cdot 10^7 \text{ N} \cdot \text{m}$. Poisson's ratio is equal to $\nu_x = 0.2$ and the mass per unit area is equal to $\mu = 1414 \text{ kg/m}^2$. The plate is subjected to the concentrated force of magnitude $P = 100\,000 \text{ N}$ moving along axis x with constant speed $v = 40 \text{ m/s}$. Figures 7 and 8 show dynamic deflections of points "a" and "b" with respect to time of the force movement along the plate. Results (continuous line) are compared with numerical results (dotted line) obtained by applying the finite element

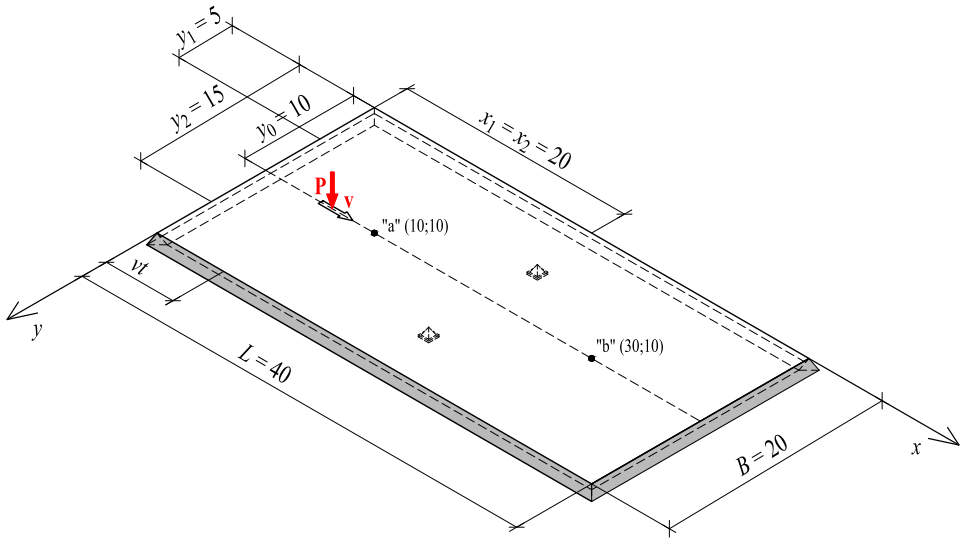


FIG. 6. Simply supported plate with two point supports subjected to a moving force.

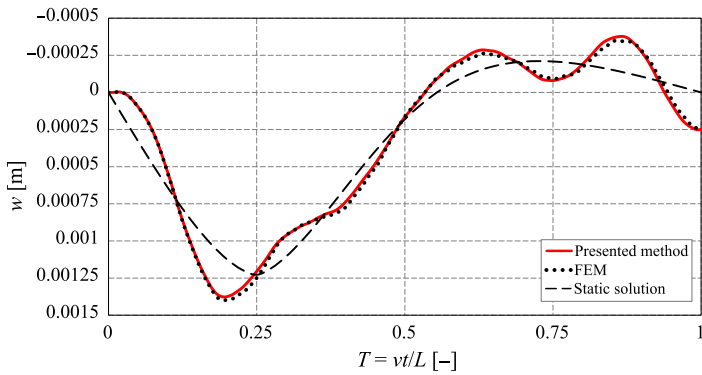


FIG. 7. Dynamic deflection of point "a".

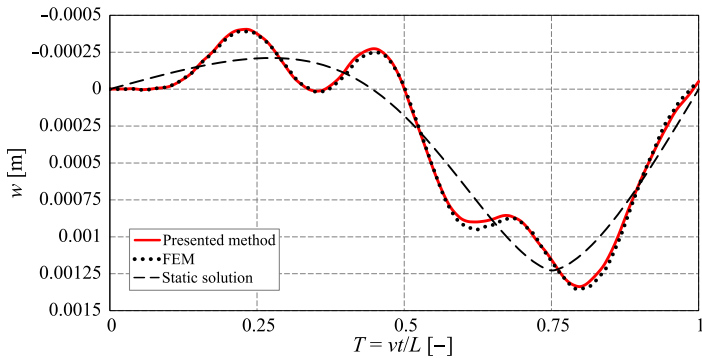


FIG. 8. Dynamic deflection of point "b".

method (FEM) and very good agreement can be observed. FEM results were obtained for spatial discretization using quadratic plate elements of size 1×1 m and time step $\Delta t = 0.0025$ s. Calculations were performed by using the Autodesk Robot Structural Analysis Professional program. The dashed black line marks the influence line of static deflection of points “a” and “b”. Figures 9 and 10 show the deformed surface of the plate at the moment when the force arrives at points “a” and “b”, respectively.

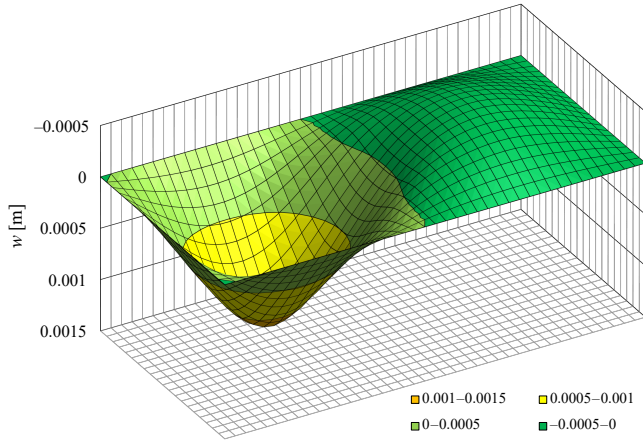


FIG. 9. Deformed surface of the plate at the moment when moving force arrives at point “a”.

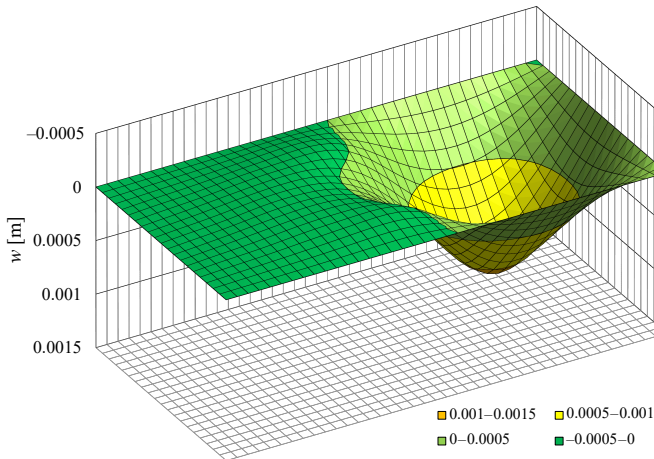


FIG. 10. Deformed surface of the plate at the moment when moving force arrives at point “b”.

4.2. Two span-bridge plate

The second example is a two-span bridge plate of dimensions shown in Fig. 11. The plate has the same rigidities and material properties as the plate

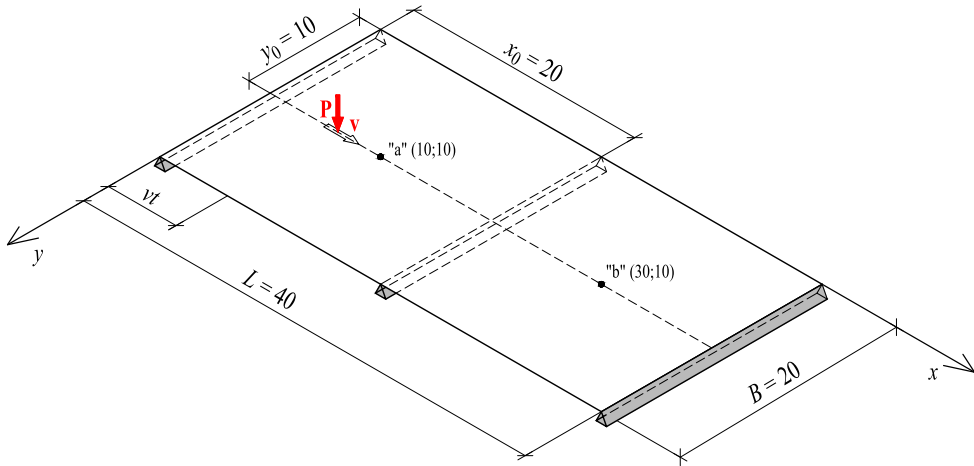


FIG. 11. Double-beam system with two elastic restraints loaded with moving point force.

in the previous example, and is also subjected to a force of the same magnitude, moving with the same speed as in the previously analyzed model. Figures 12 and 13 show dynamic deflections of points “a” and “b” with respect to time of

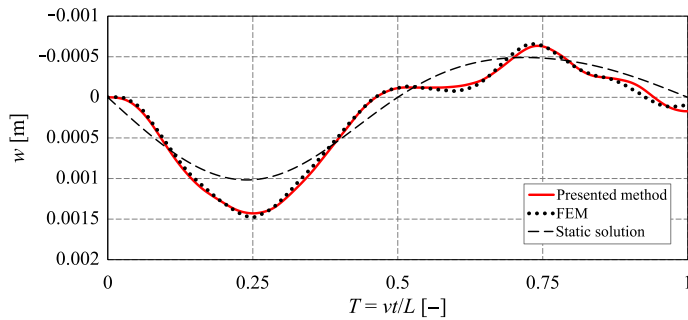


FIG. 12. Dynamic deflection of point “a”.

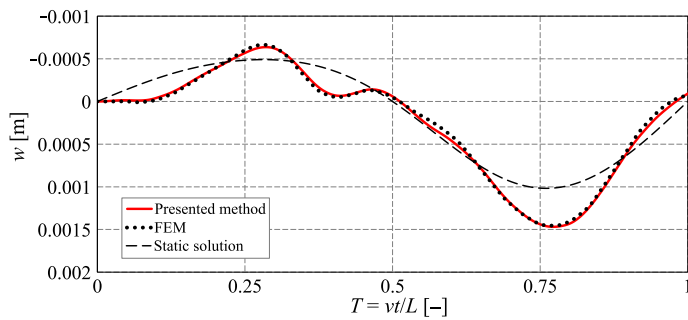


FIG. 13. Dynamic deflection of point “b”.

the force movement along the plate, respectively. Results (continuous line) are compared with numerical results (dotted line) obtained by applying the FEM and very good agreement can be observed. FEM results were obtained for spatial discretization using quadratic plate elements of size 1×1 m and time step $\Delta t = 0.0025$ s.

Calculations were performed using the Autodesk Robot Structural Analysis Professional program. The dashed black line marks the influence line of static deflection of points “a” and “b”. Figures 14 and 15 show the deformed surface of the plate at the moment when the force arrives at points “a” and “b”, respectively.

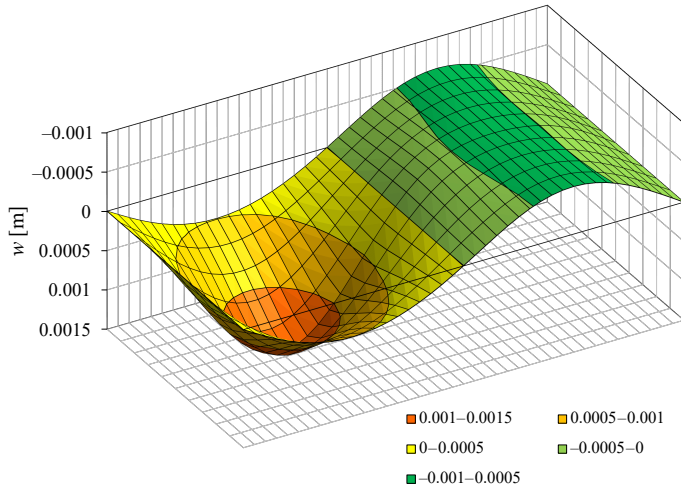


FIG. 14. Deformed surface of the plate at the moment when moving force arrives at point “a”.

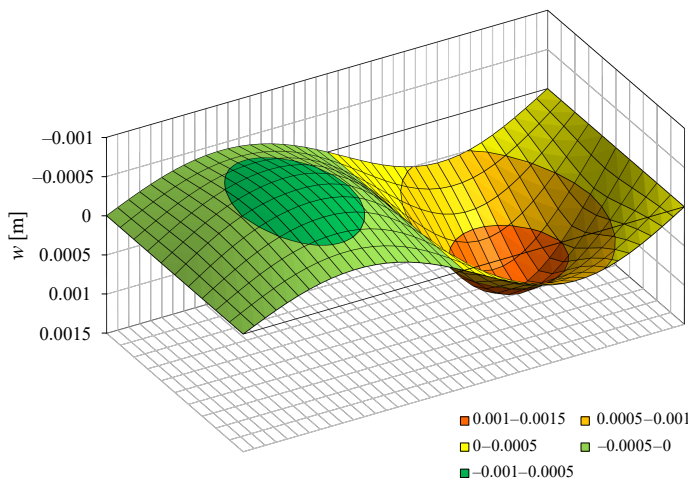


FIG. 15. Deformed surface of the plate at the moment when moving force arrives at point “b”.

5. CONCLUSION

The presented method can be successfully applied in vibration analysis of rectangular orthotropic plates with point and linear intermediate supports. After appropriate modification, the method can be applied to other types of moving non-inertial loads, such as moving distributed load or moving moment. By using the presented method, we avoid spatial discretization for a simply supported plate and discretization in the x -direction for a bridge plate. Difficulties of solving Volterra integral equations for the case of a simply supported plate can be bypassed by applying the presented numerical procedure. The effectiveness of the proposed method has been proven by comparing obtained results with those obtained by using FEM. The disadvantage of this method is that it can be applied only for non-inertial loads. Another limitation of the presented approach is that it is dedicated only to plates of rectangular shape with uniform cross-section. However, a wide group of structures fulfills these conditions, so for them, it can be applied as an alternative solution or verification for other methods.

REFERENCES

1. FARAH I., REZAIGUIA A., MOUASSA A., DEBRA L., GUENFOUD S., Free vibration analysis of multi-span orthotropic bridge deck with rubber bearings, *Diagnostyka*, **22**(1): 11–21, 2021, doi: 10.29354/diag/132209.
2. FRÝBA L., *Vibrations of Solids and Structures under Moving Load*, Telford, London, 1999.
3. KLASZTORNY M., Dynamic strength of orthotropic spans of highway bridges [in Polish: Dynamiczne wytrzymaenie ortotropowych przeseł mostów drogowych], *Archives of Civil Engineering*, **24**(4): 539–555, 1978.
4. LANGER J., Application of Legendre polynomials to the solution of the orthotropic bridge plate [in Polish: Zastosowanie wielomianów Legendre'a do rozwiązywania ortotropowej płyty mostowej], *Archives of Civil Engineering*, **22**(1): 43–55, 1966.
5. LANGER J., *Dynamics of structures* [in Polish: *Dynamika budowl*], Wrocław University of Technology Publishing House, Wrocław, 1980.
6. LAW S.S., BU J.Q., ZHU X.Q., CHAN S.L., Moving load identification on a simply supported orthotropic plate, *International Journal of Mechanical Sciences*, **49**(11): 1262–1275, 2007, doi: 10.1016/j.ijmecsci.2007.03.005.
7. LEISSA A., *Vibration of Plates*, NASA Sp-160, Washington, 1969.
8. LENARTOWICZ A., GUMINIAK M., Free vibrations of iso- and orthotropic plates considering plate variable thickness and interaction with water, *Vibrations in Physical Systems*, **31**(2): 2020216, 2020, doi: 10.21008/j.0860-6897.2020.2.16.
9. MARTÍNEZ-RODRIGO M.D., MOLINER E., ROMERO A., DE ROECK G., GALVÍN P., Maximum resonance and cancellation phenomena in orthotropic plates traversed by moving loads: Application to railway bridges, *International Journal of Mechanical Sciences*, **169**: 105316, 2020, doi: 10.1016/j.ijmecsci.2019.105316.

10. PAPKOV S.O., Vibrations of a rectangular orthotropic plate with free edges: analysis and solution of an infinite system, *Acoustical Physics*, **61**(2): 136–143, 2015, doi: 10.1134/S106377101501008X.
11. TIMOSHENKO S., WOINOWSKY-KRIEGER S., *Theory of Plates and Shells*, McGraw-Hill Book Company, New York, 1959.
12. ZAKĘŚ F., ŚNIADY P., Application of Volterra integral equations in dynamics of multispan uniform continuous beams subject to a moving load, *Shock and Vibration*, **2016**: Article ID 4070627, 2016, doi: 10.1155/2016/4070627.
13. ZHANG Y., ZHANG S., Free transverse vibration of rectangular orthotropic plates with two opposite edges rotationally restrained and remaining others free, *Applied Sciences*, **91**(1), 22, 2019, doi: 10.3390/app9010022.

Received December 30, 2022; accepted version May 17, 2023.



Copyright © 2023 The Author(s).

This is an open-access article distributed under the terms of the Creative Commons Attribution-ShareAlike 4.0 International (CC BY-SA 4.0 <https://creativecommons.org/licenses/by-sa/4.0/>) which permits use, distribution, and reproduction in any medium, provided that the article is properly cited. In any case of remix, adapt, or build upon the material, the modified material must be licensed under identical terms.